

## Supporting Information

### Compact and Filter-Free Luminescence Biosensor for Mobile *in Vitro* Diagnoses

Chen-Han Huang,<sup>†,‡</sup> Yong Il Park,<sup>†,§</sup> Hsing-Ying Lin,<sup>†</sup> Divya Pathania,<sup>†</sup> Ki Soo Park,<sup>†</sup> Maria Avila-Wallace,<sup>⊥</sup> Cesar M. Castro,<sup>†,#</sup> Ralph Weissleder,<sup>\*,†,∇</sup> and Hakho Lee<sup>\*,†</sup>

<sup>†</sup> Center for Systems Biology, Massachusetts General Hospital, Harvard Medical School, Boston, Massachusetts 02114, United States

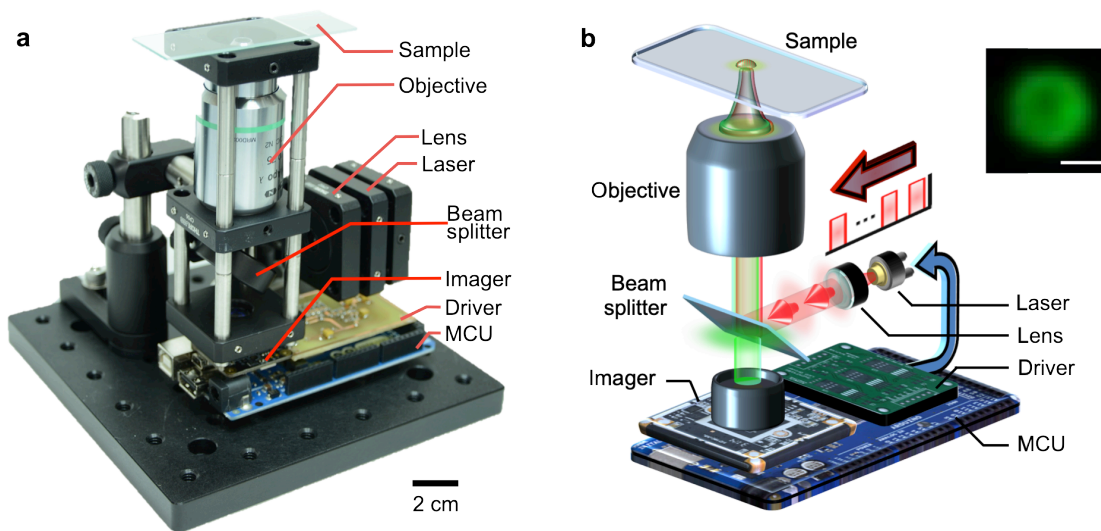
<sup>‡</sup> Department of Biomedical Sciences and Engineering, National Central University, No. 300, Zhongda Rd., Zhongli District, Taoyuan City 32001, Taiwan

<sup>§</sup> School of Chemical Engineering, Chonnam National University, 77 Yongbong-ro, Buk-gu, Gwangju 61186, Republic of Korea

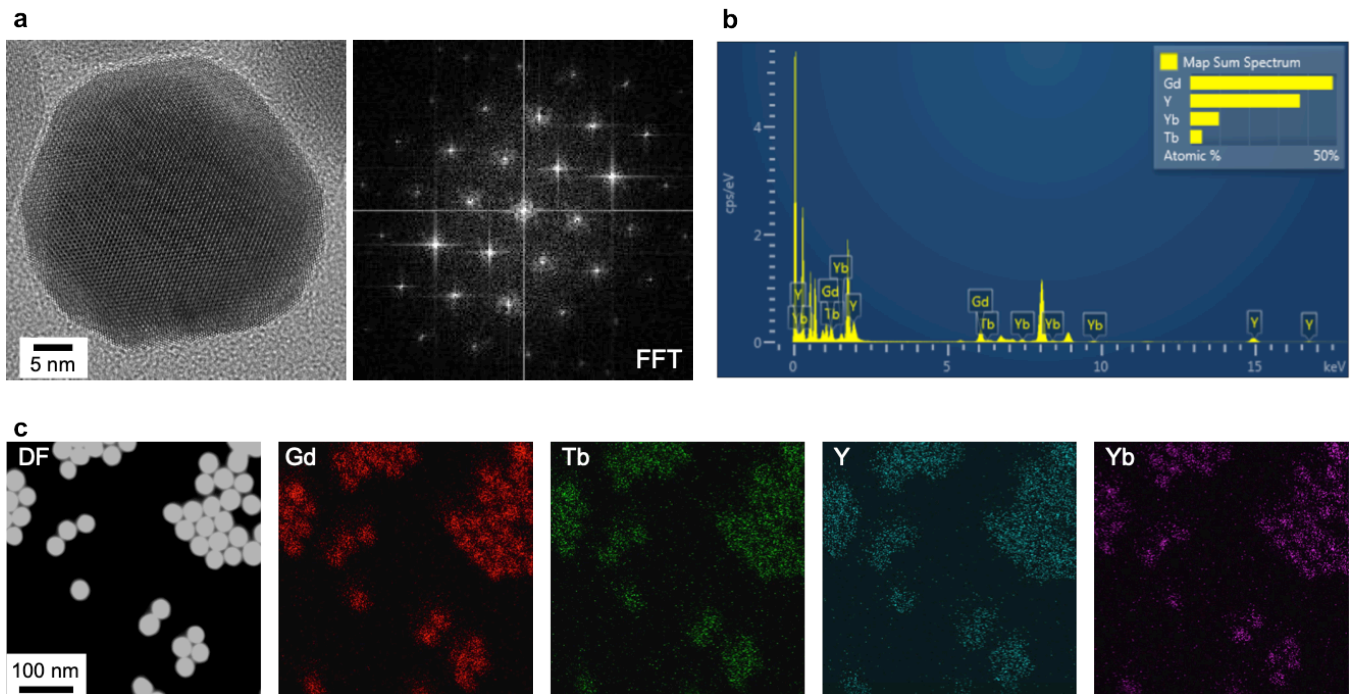
<sup>⊥</sup> Department of Obstetrics and Gynecology, Massachusetts General Hospital, Boston, Massachusetts 02114, United States

<sup>#</sup> Department of Medicine, Massachusetts General Hospital, Harvard Medical School, Boston, Massachusetts 02114, United States

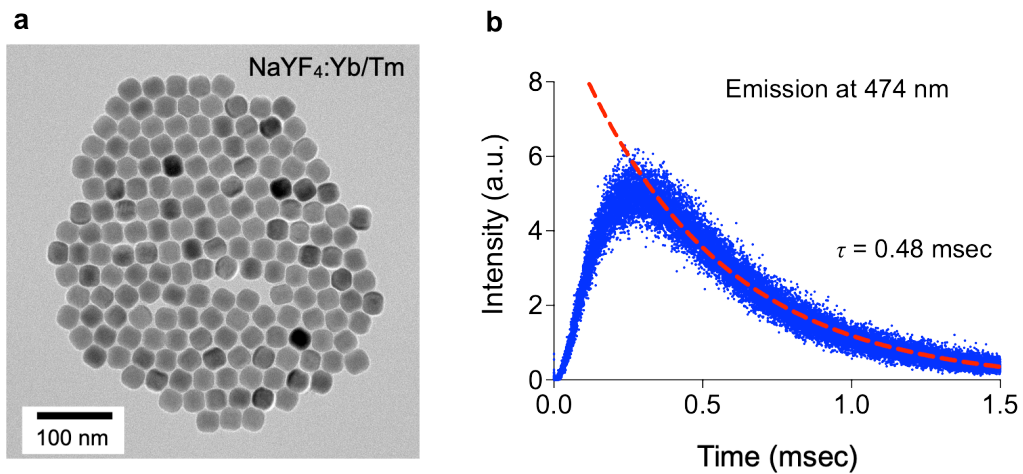
<sup>∇</sup> Department of Systems Biology, Harvard Medical School, 200 Longwood Ave, Boston, Massachusetts 02115, United States



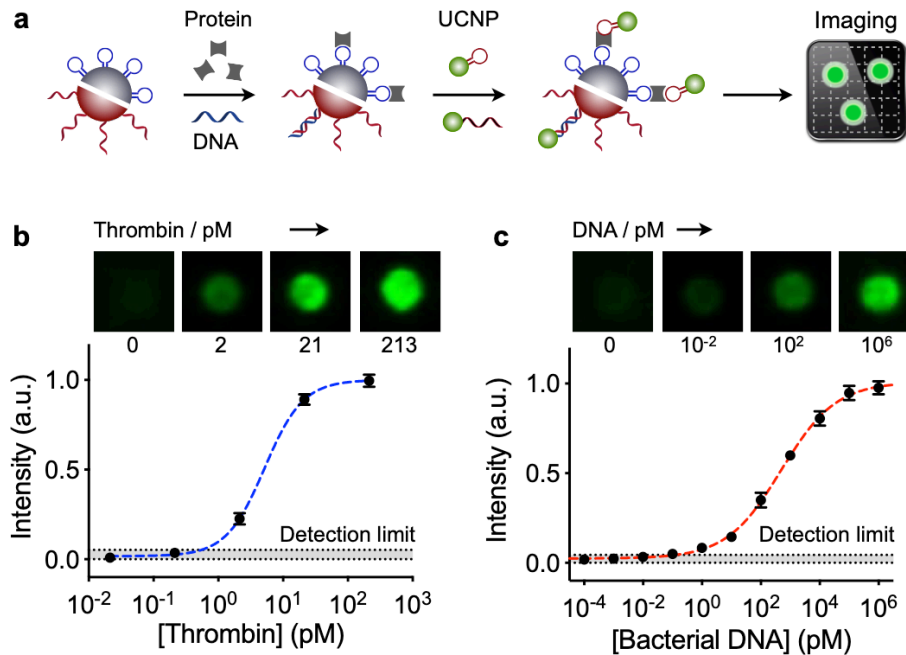
**Supplementary Figure 1. Standalone LUCID device. (a)** Device photo. The system used a CMOS imager as a detector. An epi-illumination configuration was employed to minimize system size. **(b)** Device schematic. A microcontroller unit (MCU) executed the time-gated luminescence imaging. The inset shows an acquired image of a microbead (diameter, 10  $\mu\text{m}$ ) coated with UCNPs. Scale bar, 5  $\mu\text{m}$ .



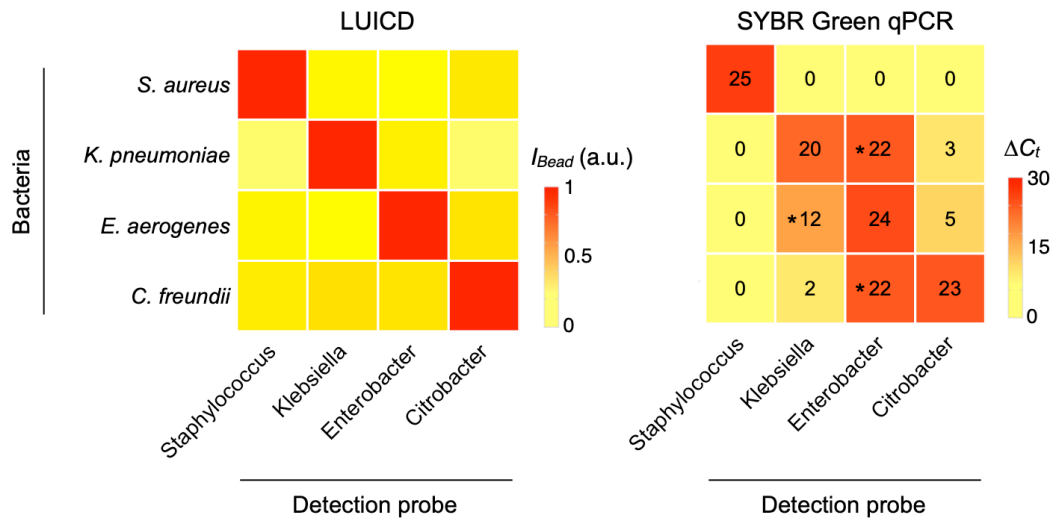
**Supplementary Figure 2. Microscopic and elemental analyses of UCNPs.** (a) High-resolution TEM (HRTEM) image of  $\text{NaGdF}_4:\text{Yb/Tm}@\text{NaGdF}_4:\text{Tb}@\text{NaYF}_4$  UCNPs (left). Fast Fourier transform (FFT; right) revealed high crystallinity of the core-shell nanoparticles. (b, c) Energy dispersive X-ray spectroscopy (b) and element mappings (c) confirmed the incorporation of key elements (e.g., Gd, Tb, Y, Yb) in particles. DF; dark-field.



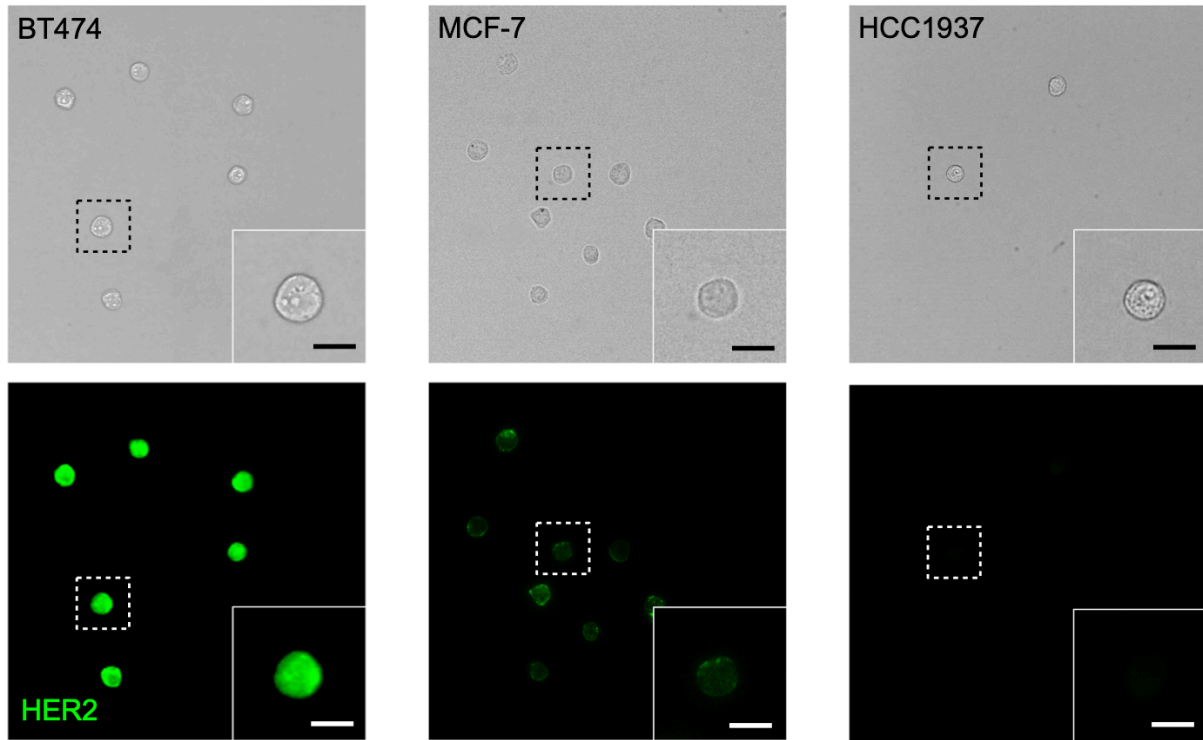
**Supplementary Figure 3. Luminescence lifetime of conventional UCNPs. (a)** TEM image of 30 nm-sized NaYF<sub>4</sub>:Yb/Tm UCNPs. **(b)** Time-resolved emission spectrum of NaYF<sub>4</sub>:Yb/Tm UCNPs monitored at 474 nm. The decay time was 0.48 msec.



**Supplementary Figure 4. LUCID assay for soluble molecular targets.** **(a)** Microbeads (diameter,  $10\ \mu\text{m}$ ) conjugated with affinity ligands captured targets, and were further labeled with target-specific UCNPs. **(b)** Thrombin detection. Microbeads and UCNPs were conjugated with thrombin-specific aptamers. The luminescence intensity varied according to the thrombin concentration (inset). We used the average intensity from 25 beads as an analytical measure. The titration experiment established the limit of detection (LOD) of  $0.5\ \text{pM}$ . Intensity was normalized to the saturation value. Data are displayed as mean  $\pm$  s.d. **(c)** Similar to the protein assay, we adopted the UCNP system to detect bacterial DNA. Microbeads and UCNPs were conjugated with oligonucleotides complementary to target DNA. The LOD was  $0.1\ \text{pM}$ . Intensity was normalized to the saturation value. Data are displayed as mean  $\pm$  s.d.



**Supplementary Figure 5. Comparison of bacteria detection.** Target cDNAs were obtained by reverse transcription of each bacterial 16S rRNA and detected by LUCID (left) and SYBR green-based quantitative PCR (qPCR; right). The same primers (**Supplementary Table 2**) were used for both assays. False positives (indicated by asterisk, \*) were observed in the SYBR-qPCR assay, that were likely due to the primer-dimer formation.



**Supplementary Figure 6. Cell profiling with LUCID.** A panel of breast cancer cell lines with varying HER2 expression were labeled with UCNPs conjugated with HER2 antibodies. Both brightfield and luminescence images were acquired by the mobile LUCID device. Scale bar, 20  $\mu\text{m}$ .

**Supplementary Table 1. Aptamer sequences used for thrombin detection.**

Target	Strand name	Aptamer sequence (5' - 3')
<i>Thrombin</i>	Capture probe	TTTTTTTTTTTTTTTTTTTTGGTTGGTGTGGTTGG
	Detection probe	AGTCCGTGGTAGGGCAGGTTGGGGTGACT

**Supplementary Table 2. DNA sequences used for bacterial detection.**

Target	Strand name	DNA sequence (5' - 3')
<i>Staphylococcus</i>	Amplicon	GGGAAGAACATATGTGTAAGTAACTGTGCACATCTTGACGGTACC TAATCAGAAAGCCACGGCTAACTAC
	Limiting primer	GTAGTTAGCCGTGGCTTTCT
	Excess primer	GGGAAGAACATATGTGTAAGTA
	Capture probe	CTTACACATATGTTCTTCCAAAAAA
	Detection probe	AAAAAATAGTTAGCCGTGGCTTTCT
<i>Klebsiella</i>	Amplicon	ACGGCAGTTAGCCGGTGCTTCTTCTGCGGGTAACGTCCAATCGC CAAGGTTATTAACCTTATCGCCTTGCCTCC
	Limiting primer	GGAGGCAAGGCGATAAGGT
	Excess primer	ACGGCAGTTAGCCGGTGCTTCT
	Capture probe	AAAAAAGAGGCAAGGCGATAAGGT
	Detection probe	AGAAGCACCGGCTAACTGCAAAAAA
<i>Enterobacter</i>	Amplicon	ACGGAGTTAGCCGGTGCTTCTTCTGCGAGTAACGTCAATCGCTAA GGTTATTAACCTTAACGCCTTCCTCC
	Limiting primer	GGAGGAAGGCGTTAAGGTTA
	Excess primer	ACGGAGTTAGCCGGTGCTTCT
	Capture probe	AAAAAAGAGGAAGGCGTTAAGGTTA
	Detection probe	AAGCACCGGCTAACTCCGAAAAAA
<i>Citrobacter</i>	Amplicon	ACGGAGTTAGCCGGTGCTTCTTCTGCGAGTAACGTCAATTGCTGC GGTTATTAACCACAACACCTTCCTCC
	Limiting primer	GGAGGAAGGTGTTGTGGTTA
	Excess primer	ACGGAGTTAGCCGGTGCTTCT
	Capture probe	AAAAAAGAGGAAGGTGTTGTGGTTA
	Detection probe	AAGCACCGGCTAACTCCGAAAAAA



## Supplementary Note.

### 1. Photon flux to a single pixel from an UCNP

- Quantum ( $Q$ ) yield of UCNP:  $\sim 0.001$  (Ref. [1])
- Absorption cross-section ( $A$ ) of  $\text{Yb}^{3+}$ :  $2.5 \times 10^{-19} \text{ cm}^2$  (Ref. [2])
- Estimated number ( $N$ ) of  $\text{Yb}^{3+}$  atoms per UCNP:  $2.8 \times 10^4$
- Incident light photon flux ( $I$ ):

$$200 \text{ mW (input)} / 1.2 \times 10^{-3} \text{ cm}^2 \text{ (illumination area)} = 1.6 \times 10^2 \text{ W/cm}^2 \approx 8 \times 10^{20} \text{ photon/cm}^2/\text{sec}$$

- Emitted photon flux from a single UCNP ( $P_0$ ):  $F = N \times A \times Q \times I = 5.7 \times 10^3 \text{ photon/sec}$

### 2. Signal-to-noise ratio (SNR) per pixel

The SNR is estimated as

$$SNR = U / (U + D \cdot t + N_r^2)^{0.5}$$

where  $U$  is the number of electrons generated by light incidence,  $D$  is the dark current,  $N_r$  is the read noise of a camera, and  $t$  is the acquisition time ( $= 3 \cdot \tau$ ).  $U$  can be further estimated as

$$U = Q_e \cdot P_0 \cdot \int_0^{3\tau} e^{-t/\tau} dt \approx Q_e \cdot P_0 \cdot \int_0^{\infty} e^{-t/\tau} dt = Q_e \cdot P_0 \cdot \tau$$

where  $Q_e$  is the quantum efficiency of the camera,  $P_0$  is the initial photon flux from an UCNP particle, and  $\tau$  is the luminescence lifetime. For reliable particle detection, we impose that  $SNR \geq 1$ , which leads to the following criterion:

$$\tau \geq \frac{(Q_e P_0 + 3D) + \sqrt{(Q_e P_0 + 3D)^2 + 4N_r^2 Q_e^2 P_0^2}}{2Q_e^2 P_0^2}$$

For a typical CMOS camera, general values are  $Q_e \sim 0.5$ ,  $D \sim 30 \text{ electron/sec}$ , and  $N_r \sim 3 \text{ (electron)}^{0.5}$ . Using these values, we obtain  $\tau \geq 1.3 \text{ msec}$ . The required  $\tau$  is thus in the range of millisecond.

## Supplementary references

- [1] Wilhelm, S. Perspectives for Upconverting Nanoparticles. *ACS Nano* **2017**, *11*, 10644-10653.
- [2] Huang, F.; Liu, X.; Ma, Y.; Kang, S.; Hu, L.; Chen, D. Origin of Near to Middle Infrared Luminescence and Energy Transfer Process of  $\text{Er}^{3+}/\text{Yb}^{3+}$  co-Doped Fluorotellurite Glasses Under Different Excitations. *Sci Rep* **2015**, *5*, 8233.